



Cite this: *RSC Adv.*, 2025, **15**, 8207

Received 9th January 2025
 Accepted 10th March 2025

DOI: 10.1039/d5ra00229j
rsc.li/rsc-advances

Towards the activity of twisted acyclic amides†

Michele Tomasini, ^{ab} Lucia Caporaso, ^b Michal Szostak^{*c} and Albert Poater ^{*a}

N,N-Boc₂ amides have emerged as the most common class of acyclic twisted amides that have been engaged in a range of C–N activation and cross-coupling processes of ubiquitous amide bonds. These amides are readily synthesized from primary amides through a site-selective *tert*-butoxycarbonylation. Due to the steric bulk of di-*tert*-butoxy groups, these amides exhibit significant C=N bond twisting, which promotes N–C bond cleavage, facilitating their use in cross-coupling reactions. Herein, we present a computational blueprint for the C=N bond rotation in *N,N*-Boc₂ amides, revealing that the rotational barrier and twist angle (τ) are influenced by the nature of the substituents at the sp² carbon position. Sterically hindered substituents exhibit the highest distortions, leading to lower rotation barriers. Rotation along the C=N bond is accompanied by phenyl ring rotation to minimize steric clashes. A strong correlation between the rotational barriers and the HOMO energies is observed. These findings provide key insights into the fundamental role of amide bond distortion in C–N activation processes.

Introduction

The amide bond is one of the most significant functional groups in both chemistry and biology.^{1,2} Historically, the Pauling resonance theory³ predicted that amides are predominantly planar structures, as confirmed by Density Functional Theory (DFT) calculations,⁴ and it has been extensively studied in chemistry, biochemistry, structural biology and materials science. The reason is that the planar nature of amides significantly influences the chemical reactivity, structural stability, and their properties. For example, inactivated amides exhibit an extremely slow rate of neutral hydrolysis, with a half-life of approximately 500 years,⁵ and the planarity of amide bonds plays a pivotal role in the formation of secondary structures like the α -helix in proteins. The chemical properties of amides, such as their preference for *O*-protonation, are also tightly linked to their planar geometry.⁶

Numerous studies have demonstrated that any deviation from planarity in amides dramatically alters their stability and reactivity.⁷ Amide bond twisting,^{8,9} in particular, has been shown to play a key role in various biological and chemical processes. For instance, it is central to enzymatic reactions such as *cis-trans* isomerization,^{10,11} amide hydrolysis,¹² and protein

splicing.¹³ More recently, it has been suggested that amide bond twisting is involved in protein *N*-glycosylation mechanisms and is a crucial factor in selective amide bond activation for cross-coupling reactions.¹⁴ This highlights the potential of exploiting amide bond twists as a valuable tool in modern synthetic organic chemistry.^{15–17}

The most common approach for inducing significant twisting in amide bonds involves embedding the amide group into rigid cyclic ring systems.¹⁸ These bicyclic bridgehead lactams possess extreme geometric distortions,¹⁹ with Winkler–Dunitz parameters showing amide bond twisting angles (τ) as high as 90° and nitrogen pyramidalization (χ_N) values up to 60°.²⁰ However, synthesizing these highly twisted amides is notoriously difficult due to the substantial reduction in amide resonance stabilization,²¹ as demonstrated by the challenges in synthesizing 2-quinuclidonium tetrafluoroborate and 1-aza-2-adamantanone.^{22,23} In fact, these latter ones often involve complex and non-trivial transformations.

In recent years, researchers have explored alternative strategies to induce amide bond twisting. In particular, Kumagai, Shibasaki, and colleagues introduced a novel class of nonplanar amides with predominantly pyramidalized amide bonds achieved through peripheral coordination of Pd(II) to nitrogen-based Lewis bases.²⁴ This method generated amides with significant distortions from planarity, exhibiting χ_N values of up to 56° and τ of 190°. However, the need for metal coordination adds complexity to the distortion of common acyclic amides. Other approaches, such as the development of *N*-tetramethylpiperidine (TMP),²⁵ *N*-glutarimide,²⁶ and *N*-1,3-thiazolidine-2-thione amides,²⁷ have provided access to nonplanar amide geometries. Unfortunately, these methods often involve derivatives from carboxylic acids and suffer from issues like high hydrolysis susceptibility, as seen with TMP amides.

^aInstitut de Química Computacional i Catalisi, Departament de Química, Universitat de Girona, C/Maria Aurèlia Capmany 69, 17003 Girona, Catalonia, Spain. E-mail: albert.poater@udg.edu

^bDipartimento di Chimica e Biologia, Università di Salerno, Via Ponte don Melillo, 84084, Fisciano, Italy

^cDepartment of Chemistry, Rutgers University, 73 Warren Street, Newark, NJ 07102, USA. E-mail: ms2223@newark.rutgers.edu

† Electronic supplementary information (ESI) available: Computational details and all *XYZ* coordinates, absolute energies of all computed species. See DOI: <https://doi.org/10.1039/d5ra00229j>



In 2018, Szostak and coworkers reported the synthesis and structural analysis of *N,N*-di-Boc amides, prepared directly from common benzamides *via* selective *N,N*-di-*tert*-butoxy carbonylation under mild conditions.²⁸ This one-step process induces significant twisting of the amide bond, which is directly applicable to primary amides²⁹ that are prevalent in organic synthesis and pharmaceutical industry.³⁰ At present, *N,N*-Boc₂ amides have been established as the most common class of acyclic twisted amides that have been engaged in a range of C–N activation and cross-coupling processes of ubiquitous amide bonds.^{14–17} From a structural standpoint, *N,N*-Boc₂ amides serve as models for exploring amide bond distortion, offering a straightforward approach to induce non-planarity.^{28–31} The di-Boc strategy effectively distorts the primary amide bond, offering valuable insights into the geometry and reactivity of twisted amides,³¹ with potential applications in organic and pharmaceutical chemistry³² as well as in biochemistry, organic synthesis, and the design of molecular switches.³³

In this manuscript, we present a computational blueprint for the C=N bond rotation in *N,N*-Boc₂ amides, at the B3LYP-D3/6-311++G(d,p)(SMD(toluene))//B3LYP-D3/6-311++G(d,p) level of theory. These findings provide key insights into the fundamental role of amide bond distortion in C–N activation processes. The study introduces a novel approach to achieve significant amide bond twisting in acyclic amides *via* simple di-*tert*-butoxy carbonylation. This method allows for the controlled and reversible distortion of amide bonds, opening up new predictive avenues,^{34,35} for the study and application of nonplanar amides in various disciplines. In particular, our research offers a new approach to inducing nonplanarity in amides without relying on complex ring systems, positioning these amides as acyclic twisted structures.

Computational details

Computational details: All DFT calculations were carried out with the Gaussian 16 set of programs.³⁶ The electronic configuration of the molecular systems was depicted using the hybrid GGA functional developed by Becke, Lee, Parr and Yang (B3LYP),^{37,38} using the Ahlrichs basis set 6-311++G(d,p).³⁹ As corrections stemming from dispersion play a crucial role in studying reactivity, we have incorporated them using Grimme's GD3 method.⁴⁰ Geometry optimizations were conducted without symmetry constraints, and the characterization of the stationary points was accomplished through analytical frequency calculations. These frequencies were employed for computing unscaled zero-point energies (ZPEs), thermal corrections, and entropy effects at 298.15 K and 1 atm. Solvent effects were estimated with the universal solvation model SMD from Cramer and Truhlar using toluene as solvent.^{41,42} The reported Gibbs energies were obtained at the B3LYP-D3/6-311++G(d,p)(SMD(toluene))//B3LYP-D3/6-311++G(d,p) level of theory. In addition, to point out that scans of any group that could rotate were performed. Moreover, we performed a total of 1 ns of MD simulations with Langevin thermostat at 1000 K for each compound by using the Atomic Simulation Environment (ASE) and the Preferred Potential (PFP).⁴³ A total of 100

snapshots per simulation were minimized following the same minimization protocol described previously. The lowest energy-minimized snap was used for quantum mechanics calculations.

Results and discussion

Starting from acyclic *N,N*-Boc₂ amides, the steric hindrance of di-*tert*-butoxy groups was studied as shown in Table 1. In detail, these amides exhibit significant twisting of the C=N bond, promoting N–C bond cleavage. The computational analysis is based on the C=N bond rotation for a series of amides in this class.⁴⁴ The entries differ in their substituents at the sp² carbon position, and with the exception of sterically hindered groups, particularly *t*Bu in entry 4, they exhibit a significant twist angle (τ). The amide with a *tert*-butyl group (entry 4) shows a large distortion, with τ values of 73.5°, to avoid steric clashes between the *tert*-butyl groups. Significant distortions ($\tau > 30^\circ$) are also observed in entries 6–13, which have different substituents in the *para* position of the phenyl ring.

As reported previously, these amides are highly destabilized, with Winkler–Dunitz parameters (τ) ranging from 35.0° to 51.3°. The twist angle (τ) is influenced primarily by electron-donating groups (EDGs), with entries 7 and 8 showing more twisting than the unsubstituted amide (entry 6). In contrast, the presence of halides induces a distortion similar to that in entry 6, while purely electron-withdrawing groups (EWGs), as in entries 11–13, reduce the τ value. Finally, the different substituents on the phenyl ring do not significantly affect the nitrogen hybridization (χ_N), which is generally more influenced by bulky groups attached to the carbonyl group of the amide bond.

A detailed analysis of C=N bond rotation was conducted for each entry in Table 1, with the resulting activation energy barriers ranging from 0.0 to 10.9 kcal mol^{–1}. As reported in the literature, amide bond rotation occurs through two possible transition states: TS-*anti* and TS-*syn*,^{45–47} where the nitrogen adopts sp³ hybridization. As illustrated in Fig. 1, these two transition states differ based on the position—*anti* or *syn*—of the lone pair orbital lobe relative to the C=O bond. The TS-*anti*

Table 1 Rotational barrier of amide bond for different *N,N*-Boc₂ amides (in kcal mol^{–1}) and relative Winkler–Dunitz parameters and % V_{Bur}

Entry	R	ΔG^\ddagger	τ	χ_N	$\Sigma\tau + \chi_N$	% V_{Bur}
1	H	8.5	1.9	1.4	3.3	59.3
2	Me	3.8	2.5	2.0	4.5	67.3
3	<i>i</i> Pr	2.7	4.6	1.3	3.4	75.8
4	<i>t</i> Bu	0.5	73.5	10.7	84.2	82.8
5	CF ₃	3.1	28.9	14.4	43.2	76.9
6	Ph	4.4	40.8	13.7	54.5	81.8
7	4-NMe ₂ Ph	9.1	51.3	11.4	62.7	81.7
8	4-OMePh	5.8	45.5	13.2	58.7	81.6
9	4-FPh	4.7	41.6	14.0	55.6	81.5
10	4-ClPh	4.3	40.0	14.1	54.1	81.7
11	4-CF ₃ Ph	3.5	36.8	14.3	51.1	81.7
12	4-CNPh	3.6	36.9	14.4	51.3	81.6
13	4-NO ₂ Ph	3.1	35.0	14.3	49.3	81.6



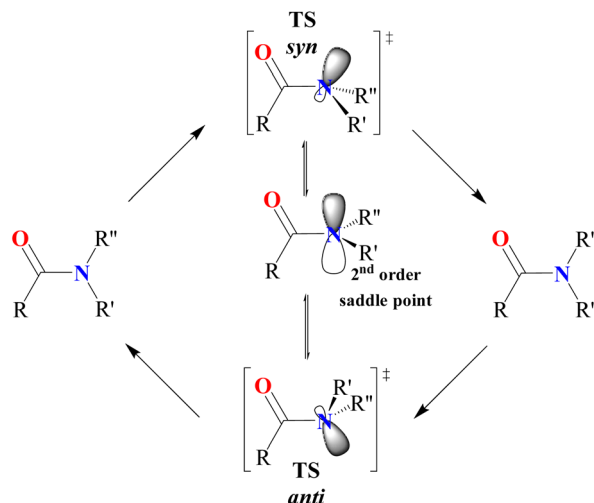


Fig. 1 Classical mechanism of *cis*–*trans* isomerization for amides.

and TS-*syn* can interconvert *via* a second-order saddle point, where the nitrogen is in an sp^2 hybridized state.

However, in this class of amides, the C=N bond rotation behaves differently. The presence of *N,N*-Boc₂ groups and the resulting delocalization of the nitrogen lone pair onto the Boc carbonyl make the rotation transition state more akin to the expected second-order saddle point, particularly for entries 1–5. The highest energy barrier ($\Delta G^\ddagger = 8.5$ kcal mol⁻¹) is observed for *N,N*-Boc₂ formamide (entry 1), where the substituent at the *C* position is a simple hydrogen atom. This causes the amide to remain nearly planar, as indicated by the Winkler–Dunitz parameters ($\tau = 1.9^\circ$ and $\chi_N = 1.4$). This planarity strengthens the C=N bond, making rotation more difficult, since amide bonds tend to be planar for the resonance stabilization due to the nitrogen lone pair and the carbonyl group.⁴⁸ Nevertheless, this planarity can be disrupted with more bulky substituents. This effect was comprehensively studied by means of % V_{Bur}

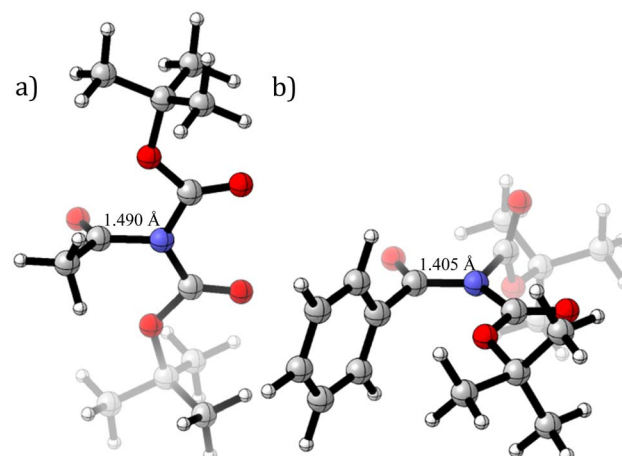


Fig. 3 C-N rotation transition states for (a) entries 2 and (b) 6 in Table 1.

index of Cavallo and coworkers.^{49,50} In detail, as progressively bulkier substituents are introduced (entries 2–5), steric clashes between the substituents increase (Fig. 2), leading to a corresponding increase in the twist angle τ (reaching 73.5° with a *tert*-butyl group in entry 4) and making rotation around the C-N bond easier. The combination of intermediate and transition-state stabilization significantly lowers the rotation barrier, particularly in the case of the *tert*-butyl group (entry 4).

On the other hand, *N,N*-Boc₂ benzamides (entries 6–13) behave differently.⁵¹ Rotation around the C-N bond induces rotation of the phenyl group around the C(phenyl)–C(carbonyl) bond. This allows the amide bond to remain planar while minimizing steric clashes between the phenyl ring and the *tert*-butoxy group, as illustrated in Fig. 3.

As a result, in transition state (TS) structures the twist angle (τ) for entries 6–13 is close to 0.0° , and the destabilization caused by increased steric hindrance is balanced by the partial restoration of amide planarity. This leads to relatively moderate activation energy barriers for rotation. Similar to τ , the rotation is hindered by electron-donating groups (EDGs) in the para position of the phenyl ring, with barriers increasing by 4.7 and

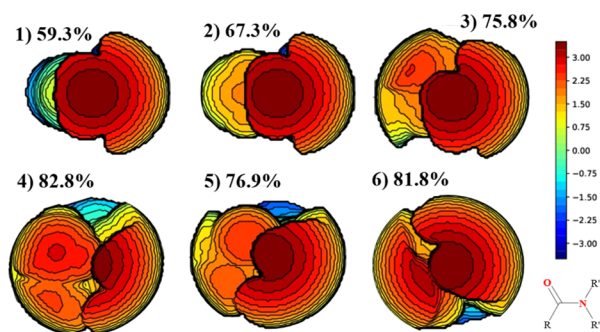


Fig. 2 Topographic steric maps (in the *xy* plane) and % V_{Bur} values were generated for the *N,N*-Boc₂ amides (entries 1–6), with a sphere radius of 3.5 Å. % V_{Bur} Represents the percent of buried volume. The centre of the sphere is defined by the midpoint between the two substituents, *R* and *R'*, with the *Z* axis passing through this point. The Boc moiety's carbon atom, bonded to the nitrogen, establishes the *xyz* plane. The steric maps are presented with isocontour curves measured in Å for a radius of 3.5 Å, providing a detailed visualization of the steric environment surrounding the amide structures.

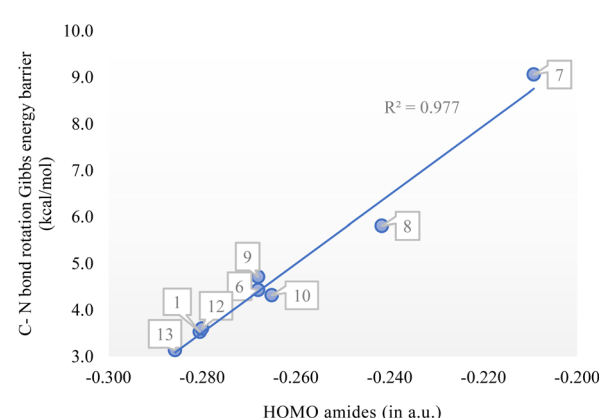


Fig. 4 Correlation between the C-N bond rotation barrier (relative Gibbs energies in kcal mol⁻¹) with the HOMO of the amides (in a.u.).



1.4 kcal mol⁻¹ for entries 7 and 8, respectively, compared to the unsubstituted phenyl (entry 4). In contrast, halides have minimal impact, with rotation barrier variations of less than 1 kcal mol⁻¹, while electron-withdrawing groups (EWGs) facilitate rotation, decreasing the barrier by up to 3.1 kcal mol⁻¹ in the presence of a nitro group (entry 13). In terms of steric hindrance, % V_{Bur} remains constant, indicating that steric effects do not contribute to the decrease in the rotation barrier. However, a strong correlation with the amides' HOMO energies was observed ($R^2 = 0.977$), as shown in Fig. 4.⁵²

Conclusions

In conclusion, this study provides a computational blueprint for understanding C=N bond rotation in *N,N*-Boc₂ amides and its dependence on steric and electronic effects. In detail, the presence of bulky di-*tert*-butoxy groups induces significant twisting of the C=N bond, which is crucial for promoting N-C bond cleavage, enhancing the reactivity of these amides in cross-coupling reactions. The rotational barriers were found to vary significantly, with the highest being observed in *N,N*-Boc₂ formamide due to its near-planar geometry. As bulkier substituents are introduced, steric clashes increase, resulting in higher twist angles and lower rotational barriers. In contrast, benzamides exhibited lower τ values and moderate activation barriers, with electron-donating groups increasing the barriers and electron-withdrawing groups lowering them. Notably, the % V_{Bur} values remained constant, indicating that steric hindrance does not contribute to the rotational barriers.

Importantly, this study identifies a strong correlation between HOMO energy levels and rotational barriers, suggesting that electronic effects are a key determinant of bond rotation. These findings provide valuable insights for the rational design of twisted amides in synthetic and pharmaceutical chemistry.

Furthermore, this work builds on past experimental data^{34,35,53} to provide a computational framework for amide bond distortion, addressing a long-standing challenge in amide activation.

Data availability

The data supporting the findings of this study are available within the article and its ESI.†

Conflicts of interest

There are no conflicts to declare.

Acknowledgements

M. S. thanks the NIH (1R35GM133326), the NSF (CAREER CHE-1650766), and Rutgers University for generous financial support. Supplement funding for this project was provided the Rutgers University – Newark Chancellor's Research Office. A. P. is a Serra Húnter Fellow and received ICREA Academia Prize 2019. A. P. thanks the Spanish Ministerio de Ciencia e

Innovación for project PID2021-127423NB-I00 and the Generalitat de Catalunya for project 2021SGR623. L. C. gratefully acknowledges financial support from CIRCC, Interuniversity Consortium Chemical Reactivity and Catalysis.

References

- 1 J. Aubé, *Angew. Chem., Int. Ed.*, 2012, **51**, 3063–3065.
- 2 C. W. Liu and M. Szostak, *Org. Biomol. Chem.*, 2018, **16**, 7998–8010.
- 3 L. Pauling, *The Nature of the Chemical Bond*, Oxford University Press, London, 1940.
- 4 (a) C. R. Kemnitz and M. J. Loewen, *J. Am. Chem. Soc.*, 2007, **129**, 2521–2528; (b) J. I. Mujika, J. M. Mercero and X. Lopez, *J. Am. Chem. Soc.*, 2005, **127**, 4445–4453; (c) J. I. Mujika, J. M. Matxain, L. A. Eriksson and X. Lopez, *Chem.-Eur. J.*, 2006, **12**, 7215–7224; (d) Z. Mucsi, A. Tsai, M. Szori, G. A. Chass, B. Viskolcz and I. G. Csizmadia, *J. Phys. Chem. A*, 2007, **111**, 13245–13254; (e) Z. Mucsi, G. A. Chass, B. Viskolcz and I. G. Csizmadia, *J. Phys. Chem. A*, 2008, **112**, 9153–9165; (f) J. Morgan, A. Greenberg and J. F. Liebman, *Struct. Chem.*, 2012, **23**, 197–199; (g) J. Morgan and A. Greenberg, *J. Chem. Thermodyn.*, 2014, **73**, 206–212; (h) J. P. Morgan, H. M. Weaver-Guevara, R. W. Fitzgerald, A. Dunlap-Smith and A. Greenberg, *Struct. Chem.*, 2017, **28**, 327–331.
- 5 V. Somayaji and R. S. Brown, *J. Org. Chem.*, 1986, **51**, 2676–2686.
- 6 C. Cox and T. Lectka, *Acc. Chem. Res.*, 2000, **33**, 849–858.
- 7 (a) H. K. Hall Jr. and A. El-Shekeil, *Chem. Rev.*, 1983, **83**, 549–555; (b) S. Yamada, *Rev. Heteroat. Chem.*, 1999, **19**, 203–236; (c) S. A. Glover, *Adv. Phys. Org. Chem.*, 2007, **42**, 35–123.
- 8 R. Szostak, S. Shi, G. Meng, R. Lalancette and M. Szostak, *J. Org. Chem.*, 2016, **81**, 8091–8094.
- 9 G. Meng, J. Zhang and M. Szostak, *Chem. Rev.*, 2021, **121**, 12746–12783.
- 10 (a) A. Williams, *J. Am. Chem. Soc.*, 1976, **98**, 5645–5651; (b) C. L. Perrin, *Acc. Chem. Res.*, 1989, **22**, 268–275.
- 11 M. Tomasini, J. Zhang, H. Zhao, E. Besalú, L. Falivene, L. Caporaso, M. Szostak and A. Poater, *Chem. Commun.*, 2022, **58**, 9950–9953.
- 12 (a) J. Liu, M. W. Albers, C. M. Chen, S. L. Schreiber and C. T. Walsh, *Proc. Natl. Acad. Sci. U. S. A.*, 1990, **87**, 2304–2308; (b) G. Fischer, *Chem. Soc. Rev.*, 2000, **29**, 119–127; (c) C. M. Eakin, A. J. Berman and A. D. Miranker, *Nat. Struct. Mol. Biol.*, 2006, **13**, 202–208.
- 13 (a) B. W. Poland, M. Q. Xu and F. A. Quiocho, *J. Biol. Chem.*, 2000, **275**, 16408–16413; (b) A. Romanelli, A. Shekhtman, D. Cowburn and T. W. Muir, *Proc. Natl. Acad. Sci. U. S. A.*, 2004, **101**, 6397–6402; (c) P. Shemella, B. Pereira, Y. M. Zhang, P. van Roey, G. Belfort, S. Garde and S. K. Nayak, *Biophys. J.*, 2007, **92**, 847–853.
- 14 (a) C. Lizak, S. Gerber, S. Numao, M. Aebi and K. P. Locher, *Nature*, 2011, **474**, 350–355; (b) C. Lizak, S. Gerber, G. Michaud, M. Schubert, Y. Y. Fan, M. Bucher, T. Darbre, M. Aebi, J. L. Reymond and K. P. Locher, *Nat. Commun.*, 2013, **4**, 2627; (c) R. Takise, K. Muto and J. Yamaguchi,

Chem. Soc. Rev., 2017, **46**, 5864–5888; (d) G. Meng, S. Shi and M. Szostak, *Synlett*, 2016, **27**, 2530–2540; (e) C. Liu and M. Szostak, *Chem.-Eur. J.*, 2017, **23**, 7157–7173; (f) J. E. Dander and N. K. Garg, *ACS Catal.*, 2017, **7**, 1413–1423.

15 S. Yang, X. Yu, Y. Liu, M. Tomasini, L. Caporaso, A. Poater, L. Cavallo, C. S. J. Cazin, S. P. Nolan and M. Szostak, *J. Org. Chem.*, 2023, **88**, 10858–10868.

16 G. Li, T. Zhou, A. Poater, L. Cavallo, S. P. Nolan and M. Szostak, *Catal. Sci. Technol.*, 2020, **10**, 710–716.

17 G. Li, P. Lei, M. Szostak, E. Casals-Cruañas, A. Poater, L. Cavallo and S. P. Nolan, *ChemCatChem*, 2018, **10**, 3096–3106.

18 M. Szostak and J. Aubé, *Chem. Rev.*, 2013, **113**, 5701–5765.

19 (a) M. Liniger, D. G. VanderVelde, M. K. Takase, M. Shahgholi and B. M. Stoltz, *J. Am. Chem. Soc.*, 2016, **138**, 969–974; (b) M. Liniger, Y. Liu and B. Stoltz, *J. Am. Chem. Soc.*, 2017, **139**, 13944–13949; (c) A. J. Kirby, I. V. Komarov, P. D. Wothers and N. Feeder, *Angew. Chem., Int. Ed.*, 1998, **37**, 785–786; (d) I. V. Komarov, S. Yanik, A. Y. Ishchenko, J. E. Davies, J. M. Goodman and A. J. Kirby, *J. Am. Chem. Soc.*, 2015, **137**, 926–930; (e) J. Golden and J. Aubé, *Angew. Chem., Int. Ed.*, 2002, **41**, 4316–4318; (f) Y. Lei, A. D. Wroblewski, J. E. Golden, D. R. Powell and J. Aubé, *J. Am. Chem. Soc.*, 2005, **127**, 4552–4553; (g) B. Sliter, J. Morgan and A. Greenberg, *J. Org. Chem.*, 2011, **76**, 2770–2781; (h) J. Artacho, E. Ascic, T. Rantanen, J. Karlsson, C. J. Wallentin, R. Wang, O. Wendt, F. M. Harmata, V. Snieckus and K. Wärnmark, *Chem.-Eur. J.*, 2012, **18**, 1038–1042.

20 F. K. Winkler and J. D. Dunitz, *J. Mol. Biol.*, 1971, **59**, 169–182.

21 F. Hu, R. Lalancette and M. Szostak, *Angew. Chem., Int. Ed.*, 2016, **55**, 5062–5066.

22 K. Tani and B. M. Stoltz, *Nature*, 2006, **441**, 731–734.

23 S. A. Glover and A. A. Rosser, *J. Org. Chem.*, 2012, **77**, 5492–5502.

24 S. Adachi, N. Kumagai and M. Shibasaki, *Chem. Sci.*, 2017, **8**, 85–90.

25 M. Hutchby, C. E. Houlden, M. F. Haddow, S. N. Tyler, G. C. Lloyd-Jones and K. I. Booker-Milburn, *Angew. Chem., Int. Ed.*, 2012, **51**, 548–551.

26 (a) G. Meng and M. Szostak, *Org. Lett.*, 2015, **17**, 4364–4367; (b) V. Pace, W. Holzer, G. Meng, S. Shi, R. Lalancette, R. Szostak and M. Szostak, *Chem.-Eur. J.*, 2016, **22**, 14494–14498.

27 (a) S. Yamada, *Angew. Chem., Int. Ed. Engl.*, 1993, **32**, 1083–1085; (b) S. Yamada, *Angew. Chem., Int. Ed. Engl.*, 1995, **34**, 1113–1115.

28 G. Meng, S. Shi, R. Lalancette, R. Szostak and M. Szostak, *J. Am. Chem. Soc.*, 2018, **140**, 727–734.

29 (a) S. D. Roughley and A. M. Jordan, *J. Med. Chem.*, 2011, **54**, 3451–3479; (b) V. R. Pattabiraman and J. W. Bode, *Nature*, 2011, **480**, 471–479; (c) A. A. Kaspar and J. M. Reichert, *Drug Discov. Today*, 2013, **18**, 807–817.

30 (a) H. Bae, J. Park, R. Yoon, S. Lee and J. Son, *RSC Adv.*, 2024, **14**, 9440; (b) C. Sivaraj and T. Gandhi, *RSC Adv.*, 2023, **13**, 9231–9236.

31 (a) G. Meng, S. Shi and M. Szostak, *ACS Catal.*, 2016, **6**, 7335–7339; (b) S. Shi and M. Szostak, *Org. Lett.*, 2016, **18**, 5872–5875; (c) G. Meng and M. Szostak, *ACS Catal.*, 2017, **7**, 7251–7256.

32 (a) A. Greenberg and C. A. Venanzi, *J. Am. Chem. Soc.*, 1993, **115**, 6951–6957; (b) A. Greenberg, D. T. Moore and T. D. DuBois, *J. Am. Chem. Soc.*, 1996, **118**, 8658–8668.

33 (a) J. Clayden, A. Lund, L. Vallverdu and M. Helliwell, *Nature*, 2004, **431**, 966–971; (b) J. Clayden, *Chem. Soc. Rev.*, 2009, **38**, 817–829; (c) J. Sola, S. P. Fletcher, A. Castellanos and J. Clayden, *Angew. Chem., Int. Ed.*, 2010, **49**, 6836–6839; (d) P. C. Knipe, S. Thompson and A. D. Hamilton, *Chem. Sci.*, 2015, **6**, 1630–1639; (e) N. Volz and J. Clayden, *Angew. Chem., Int. Ed.*, 2011, **50**, 12148–12155.

34 S. Escayola, N. Bahri-Laleh and A. Poater, *Chem. Soc. Rev.*, 2024, **53**, 853–882.

35 R. Montreal-Corona, A. Pla-Quintana and A. Poater, *Trends Chem.*, 2023, **5**, 935–946.

36 M. J. Frisch, G. W. Trucks, H. B. Schlegel, G. E. Scuseria, M. A. Robb, J. R. Cheeseman, G. Scalmani, V. Barone, G. A. Petersson, H. Nakatsuji, X. Li, M. Caricato, A. V. Marenich, J. Bloino, B. G. Janesko, R. Gomperts, B. Mennucci, H. P. Hratchian, J. V. Ortiz, A. F. Izmaylov, J. L. Sonnenberg, D. Williams-Young, F. Ding, F. Lipparini, F. Egidi, J. Goings, B. Peng, A. Petrone, T. Henderson, D. Ranasinghe, V. G. Zakrzewski, J. Gao, N. Rega, G. Zheng, W. Liang, M. Hada, M. Ehara, K. Toyota, R. Fukuda, J. Hasegawa, M. Ishida, T. Nakajima, Y. Honda, O. Kitao, H. Nakai, T. Vreven, K. Throssell, J. A. Montgomery Jr, J. E. Peralta, F. Ogliaro, M. J. Bearpark, J. J. Heyd, E. N. Brothers, K. N. Kudin, V. N. Staroverov, T. A. Keith, R. Kobayashi, J. Normand, K. Raghavachari, A. P. Rendell, J. C. Burant, S. S. Iyengar, J. Tomasi, M. Cossi, J. M. Millam, M. Klene, C. Adamo, R. Cammi, J. W. Ochterski, R. L. Martin, K. Morokuma, O. Farkas, J. B. Foresman and D. J. Fox, *Gaussian 16, Revision C.01*, Gaussian, Inc., Wallingford CT, 2016.

37 (a) A. D. Becke, *J. Chem. Phys.*, 1993, **98**, 5648–5652; (b) C. T. Lee, W. T. Yang and R. G. Parr, *Phys. Rev. B: Condens. Matter Mater. Phys.*, 1988, **37**, 785–789; (c) P. J. Stephens, F. J. Devlin, C. F. Chabalowski and M. J. Frisch, *J. Phys. Chem.*, 1994, **98**, 11623–11627.

38 (a) A. Poater, X. Ribas, A. Llobet, L. Cavallo and M. Solà, *J. Am. Chem. Soc.*, 2008, **130**, 17710–17717; (b) S. Karimi, N. Bahri-Laleh, S. Sadjadi, G. Pareras, M. Nekoomanesh-Haghghi and A. Poater, *J. Ind. Eng. Chem.*, 2021, **97**, 441–451.

39 R. Ditchfield, W. J. Hehre and J. A. Pople, *J. Chem. Phys.*, 1971, **54**, 724–728.

40 S. Grimme, J. Antony, S. Ehrlich and H. Krieg, *J. Chem. Phys.*, 2010, **132**, 154104.

41 V. Barone and M. Cossi, *J. Phys. Chem. A*, 1988, **102**, 1995–2001.

42 J. Tomasi and M. Persico, *Chem. Rev.*, 1994, **94**, 2027–2094.

43 S. Takamoto, C. Shinagawa, D. Motoki, K. Nakago, W. Li, I. Kurata, T. Watanabe, Y. Yayama, H. Iriguchi, Y. Asano, T. Onodera, T. Ishii, T. Kudo, H. Ono, R. Sawada, R. Ishitani, M. Ong, T. Yamaguchi, T. Kataoka, A. Hayashi,



N. Charoenphakdee and T. Ibuka, *Nat. Commun.*, 2022, **13**, 2991.

44 (a) A. F. Hegarty, M. T. McCormack, K. Brady, G. Ferguson and P. J. Roberts, *J. Chem. Soc., Perkin Trans. 2*, 1980, **2**, 867–875; (b) K. Brady and A. F. Hegarty, *J. Chem. Soc., Perkin Trans. 2*, 1980, (2), 121–126; (c) J. Tailhades, N. A. Patil, M. A. Hossain and J. D. Wade, *J. Pept. Sci.*, 2015, **21**, 139–147; (d) F. S. Gibson, S. C. Bergmeier and H. Rapoport, *J. Org. Chem.*, 1994, **59**, 3216–3218.

45 B. S. Thakkar, J.-S. M. Svendsen and R. A. Engh, *J. Phys. Chem. A*, 2017, **121**, 6830–6837.

46 Y. A. Mantz, D. Branduardi, G. Bussi and M. Parrinello, *J. Phys. Chem. B*, 2009, **113**, 12521–12529.

47 K. B. Wiberg, P. R. Rablen, D. J. Rush and T. A. Keith, *J. Am. Chem. Soc.*, 1995, **117**, 4261–4270.

48 G. Li, S. Ma and M. Szostak, *Trends Chem.*, 2020, **2**, 914–928.

49 L. Falivene, R. Credendino, A. Poater, A. Petta, L. Serra, R. Oliva, V. Scarano and L. Cavallo, SambVca 2. A Web Tool for Analyzing Catalytic Pockets with Topographic Steric Maps, *Organometallics*, 2016, **35**, 2286–2293.

50 L. Falivene, R. Credendino, A. Poater, A. Petta, L. Serra, R. Oliva, V. Scarano and L. Cavallo, *Organometallics*, 2016, **35**, 2286–2293.

51 P. T. Corbett, J. Leclaire, L. Vial, K. R. West, J. L. Wietor, J. K. M. Sanders and S. Otto, *Chem. Rev.*, 2006, **106**, 3652–3711.

52 (a) Z. Cao, L. Falivene, A. Poater, B. Maity, Z. Zhang, G. Takasao, S. B. Sayed, A. Petta, G. Talarico, R. Oliva and L. Cavallo, *Cell Rep. Phys. Sci.*, 2025, **6**, 102348; (b) D. Dalmau and J. V. Alegre Requena, *Wiley Interdiscip. Rev.: Comput. Mol. Sci.*, 2024, **14**, e1733.

53 (a) M. Tomasini, M. Szostak and A. Poater, *Asian J. Org. Chem.*, 2025, e202400749; (b) R. Montreal-Corona, Á. Díaz-Jiménez, A. Roglans, A. Poater and A. Pla-Quintana, *Adv. Synth. Catal.*, 2023, **365**, 760–766.

